

Normal liquid ${}^3\text{He}$ studied by Path Integral Monte Carlo with a parametrized partition function

Tommaso Morresi^{1*}, Giovanni Garberoglio^{1*}

¹ *European Centre for Theoretical Studies in Nuclear Physics and Related Areas (ECT*), Fondazione Bruno Kessler, Italy*

We compute the energy per particle of normal liquid ${}^3\text{He}$ in the temperature range $0.15 - 2$ K using Path Integral Monte Carlo simulations, leveraging a recently proposed method to overcome the sign problem – a long-standing challenge in many-body fermionic simulations. This approach is based on introducing a parameter ξ into the partition function, which allows a generalization from bosons ($\xi = 1$) to fermions ($\xi = -1$). By simulating systems with $\xi \geq 0$, where the sign problem is absent, one can then extrapolate to the fermionic case at $\xi = -1$. Guided by an independent particle model that uncovers non-analytic behavior due to the superfluid transition, which is moderated by finite-size effects, we develop a tailored extrapolation strategy for liquid ${}^3\text{He}$ that departs from the extrapolation schemes shown to be accurate in those cases where quantum degeneracy effects are weak, and enables accurate results in the presence of Bose–Einstein Condensation and superfluidity for $\xi > 0$. Our approach extends the previously proposed framework and yields energy per particle values in excellent agreement with experimental data.

I. INTRODUCTION

Computer simulations of interacting many-fermion systems are notoriously difficult due to the requirement of antisymmetric quantum states. If one aims at exact solutions (that is, avoiding uncontrolled approximations), numerical methods such as the Full Configuration Interaction scale exponentially with the system size, [1] preventing calculations to be performed except for the smallest systems. In the case of electronic structure calculations, this currently limits the size of the systems that can be studied to tens of electrons. For larger systems, approximations such as the Coupled Cluster approach provide results that are “chemically accurate” when single, double and perturbative triplet excitations are considered, at the cost of scaling with the number of electrons N as $\mathcal{O}(N^7)$. [2]

Monte Carlo methods are generally expected to provide a better scaling, but in this case the antisymmetry requirement results in the so called *sign problem*; sampling regions of positive and negative values of the density matrix results in a large variance of the various observables, [3–5] again limiting the size of the systems that can be studied. Recently, an extensive Path Integral Monte Carlo (PIMC) simulation of liquid ${}^3\text{He}$ could not exceed $N = 38$ even when resorting to large-scale computational resources. [6] Several approximations, such as the famous “fixed nodes” one, [7–9] provide good quality results with a favorable scaling of $\mathcal{O}(N^3)$ with the number of particles. [4]

In the past few years, a novel method to overcome the sign problem for many-body fermionic simulations has been introduced. This approach is based on the consideration that the quantum statistical partition function of a system of bosons and fermions differs only by the value of a single parameter, ξ , which assumes the value $\xi = 1$ for bosons and $\xi = -1$ for fermions. [10, 11] Since the partition function turns out to be a *continuous* function

of ξ , one can envision an extrapolation procedure to the fermion case, based on results in the $\xi \geq 0$ regime, where PIMC calculations are not affected by the sign problem and can be carried out with acceptable computational resources. This approach has been successfully applied to the study of the electron gas [10] and solvable fermion models. [12] In practice, one computes the average energy per particle E (or any other observable) along an isotherm of temperature T for several values of $\xi \geq 0$. These isotherms are used to compute how ξ depends on T for fixed energy E . These studies showed that simple fitting functions, usually quadratic polynomials, for $\xi_E(T)$ extrapolate very well to $\xi = -1$, thus providing the temperature T at which the fermionic system attains energy E .

In this work, we investigate how this approach can be used to compute $E(T)$ in the case of normal liquid ${}^3\text{He}$. We find that the presence of Bose–Einstein Condensation (BEC) and the accompanying superfluid transition in the $\xi > 0$ region results in a non-analytic behavior for the function $\xi_E(T)$ which, despite being smoothed out by finite-size effects, requires more care in extrapolating to $\xi = -1$ than in the case of previous studies. [12] After recalling the general theoretical framework, we will discuss an independent particle model that highlights the effect of BEC on the values of $E(T, \xi)$ along an isotherm and provides important clues on the general form of $\xi_E(T)$ in this case. Secondly, we will study finite-size effects in the same model, and investigate how they affect the extrapolation procedure. Finally, based on extensive PIMC simulations of $E(T, \xi)$, we apply our extrapolation method to compute $E(T)$ for ${}^3\text{He}$, finding a very good agreement with experimental data.

II. THEORETICAL FRAMEWORK

The quantum statistical partition function for N identical particles at temperature T can be written as

$$Z_{\pm}(T) = \frac{1}{N!} \sum_{\mathcal{P}} (\pm 1)^{\mathcal{P}} \int d\mathbf{R} \rho(\mathbf{R}, \mathcal{P}\mathbf{R}, \beta), \quad (1)$$

where $\beta = (k_{\text{B}}T)^{-1}$, k_{B} is the Boltzmann constant, the sign '+' is for bosons and '-' for fermions, and $\mathbf{R} = (\mathbf{r}_1, \mathbf{r}_2, \dots, \mathbf{r}_N)$ is a compact notation for all the particle coordinates. In Eq. (1), $\rho(\mathbf{R}, \mathbf{R}', \beta) = \langle \mathbf{R} | e^{-\beta H} | \mathbf{R}' \rangle$ is the canonical density matrix corresponding to the Hamiltonian H , and $\mathcal{P}\mathbf{R} = (\mathbf{r}_{\mathcal{P}(1)}, \mathbf{r}_{\mathcal{P}(2)}, \dots, \mathbf{r}_{\mathcal{P}(N)})$ denotes the position vectors with permuted labels.

One can generalize Eq. (1) introducing a real parameter ξ and writing

$$Z_{\xi}(T) = \frac{1}{N!} \sum_{\mathcal{P}} \xi^{N_{\mathcal{P}}} \int d\mathbf{R} \rho(\mathbf{R}, \mathcal{P}\mathbf{R}, \beta). \quad (2)$$

where $N_{\mathcal{P}}$ denotes the minimum number of times for which pairs of indices have to be interchanged in the current permutation \mathcal{P} to recover the original (diagonal) order. [10–14]

In Eq. (2), the parameter ξ interpolates continuously from bosons ($\xi = 1$), to distinguishable particles ($\xi = 0$), to fermions ($\xi = -1$), and can take any real value in $(-\infty, +\infty)$. The energy of the system described by Eq. (2) can be obtained from standard statistical mechanics considerations as

$$E_{\xi}(T) = -\frac{1}{Z_{\xi}(T)} \frac{\partial Z_{\xi}(T)}{\partial \beta}, \quad (3)$$

where the subscript means the ξ variable is kept fixed. In order to estimate the energy in the case of fermionic systems, one can then exploit the fact that both $Z_{\xi}(T)$ and $E_{\xi}(T)$ are continuous functions of T and ξ . By knowing their behavior in the $\xi \geq 0$ sector, where calculations can be performed without encountering the sign problem, one can extrapolate the value of the energy to $\xi = -1$. In fact, for $\xi \geq 0$ one can perform standard PIMC simulations [15] just by taking into account the different positive weights due to the factor $\xi^{N_{\mathcal{P}}}$ in Eq. (2).

There are two necessary conditions that can be used to guide the extrapolation to $\xi = -1$: [11]

1. $\frac{\partial E_T(\xi)}{\partial \xi} < 0$. The parameter ξ induces an effectively repulsive exchange interaction for fermions and effectively attractive exchange interaction for bosons; thus for a given fixed temperature the energy should decrease with increasing ξ .
2. $\frac{\partial E_{\xi}(T)}{\partial T} = -\frac{1}{T^2} \frac{\partial E_{\xi}(T)}{\partial \beta} > 0$. This is the condition to have a positive heat capacity.

In a first paper [11], the authors proposed a parabolic behavior of the energy with respect to ξ :

$$E(T, \xi) = c_0 + c_1 \xi + c_2 \xi^2, \quad (4)$$

for each temperature. They found that this empirical formula worked quite well for different repulsive interactions, such as the Coulomb, the dipolar and the Gaussian ones. [11] The same approach has been shown to give a good description of large Fermi-systems of weak quantum degeneracy, but it was found to break down for moderate to high quantum degeneracy. [10] Also, the parabolic extrapolation has been used for other observables such as the static structure factor. Recently, the extrapolation approach has been successfully adopted to describe warm dense hydrogen and beryllium. [13]

A more general approach was then proposed in Ref. [12]. Based on the same two physical assumptions previously mentioned, the authors generalised the theory by considering ξ as a function of both T and E . In particular, they proved the following relation:

$$\left. \frac{\partial \xi_E(T)}{\partial T} \right|_{T=0} = 0, \quad (5)$$

resulting in the lack of a the linear term when expanding ξ as a function of T , *i.e.*,

$$\xi_E(T) = a_0(E) + a_2(E)T^2 + \sum_{i>2} a_i(E)T^i. \quad (6)$$

In practice, one computes numerically $E(\xi)$ for several values of T , samples the function $\xi_E(T)$ and fits the parameters a_i using Eq. (6). Finally, the temperature T_E where the fermionic system attains energy E is obtained by solving $\xi_E(T_E) = -1$. In their analysis with free electrons, keeping only the quadratic term in Eq. (6) was enough to provide accurate results. [12]

III. INDEPENDENT-PARTICLE MODEL

Before presenting the PIMC results for ${}^3\text{He}$, let us investigate an independent-particle model system. In this case, the relation between ξ and T must be computed exactly, but some analytic considerations highlight the effect of BEC. The generalized quantum statistical mechanics as a function of ξ , that is the statistical mechanics of particles obeying the generalized commutation relation

$$a_{\mathbf{q}} a_{\mathbf{q}'}^{\dagger} - \xi a_{\mathbf{q}'}^{\dagger} a_{\mathbf{q}} = \delta_{\mathbf{q}, \mathbf{q}'}, \quad (7)$$

has been studied in Ref. 16, where it is shown that in an independent-particle model having Hamiltonian $H = \sum_{\mathbf{q}} \epsilon(\mathbf{q}) \hat{N}_{\mathbf{q}}$ (where $\hat{N}_{\mathbf{q}}$ is the usual number operator), occupation numbers have the form

$$f(\epsilon; T, \mu) = \frac{1}{\exp\left(\frac{\epsilon - \mu}{T}\right) - \xi}, \quad (8)$$

where μ is the chemical potential. In the grand canonical ensemble, one obtains the following coupled equation relating the temperature T and the chemical potential μ

to the number of particles N and the average energy E

$$N = N_c + \frac{\Omega}{(2\pi)^3} \int_0^\infty \frac{4\pi q^2}{\exp\left(\frac{\epsilon(q)-\mu}{T}\right) - \xi} dq \quad (9)$$

$$E = \frac{\Omega}{(2\pi)^3} \int_0^\infty \frac{4\pi q^2 \epsilon(q)}{\exp\left(\frac{\epsilon(q)-\mu}{T}\right) - \xi} dq, \quad (10)$$

where Ω is the volume of the system and the dispersion relation depends only on $q = |\mathbf{q}|$ due to spherical symmetry. We will assume in the following that $\epsilon(q > 0) > 0$ and that $\epsilon(q \rightarrow 0) = 0$.

The symbol N_c in Eq. (9) represents the non-zero macroscopic number of particles in the ground state (*i.e.*, the state with $\epsilon = 0$) that signals the onset of BEC, which is characterized by the fact that N_c/N remains finite in the thermodynamic limit. [17] The presence of BEC in this system is related to the fact that for any $\xi > 0$ the chemical potential has an upper bound, lest the occupation numbers of Eq. (8) become negative. Inspection of Eq. (8) shows that the chemical potential must be smaller than the critical value $\mu_c = -T \log \xi$. Conversely, if one considers Eq. (9) as a function of ξ along an isotherm, there is a critical value of the parameter ξ after which $N_c > 0$ given by

$$\xi_c = \frac{\Omega}{N(2\pi)^3} \int_0^\infty \frac{4\pi q^2}{\exp\left(\frac{\epsilon(q)}{T}\right) - 1} dq. \quad (11)$$

In correspondence to this critical value, the energy as a function of ξ exhibits non-analytic behavior due to the increasing occupation of N_c . The precise form of this non-analyticity depends on the structure of the dispersion relation $\epsilon(q)$ and takes the form

$$\frac{N_c}{N} \sim 1 - \left(\frac{T}{T_c}\right)^\alpha, \quad (12)$$

where T_c is the BEC transition temperature, while $\alpha = 3/2$ for a quadratic dispersion and $\alpha = 3$ for a linear dispersion. In the case of ^3He , the dispersion relation is closer to the linear case, which corresponds to a stronger non-analytic behavior.

In order to solve Eqs. (9) and (10), we use a dispersion relation parametrized to mimic the single-particle excitation spectrum of helium [18], which has the form

$$\epsilon(q) = \sqrt{\alpha_1 q \cdot \sin(\alpha_2 q) + \left(\frac{\hbar^2 q^2}{2m}\right)^2}, \quad (13)$$

where $m = 3.016$ a.m.u. is the mass of ^3He . We notice that by tuning the two parameters, and α_1 in particular, one can also obtain a free dispersion ($\alpha_1=0$, short dashed line in Fig. 1) or a Bogoliubov-like dispersion ($\sqrt{\alpha_1 \alpha_2 / \hbar^2} \sim 160$ [m/s]). Here the two parameters α_1 and α_2 are taken such that $\alpha_2 = 2.45$ Å and $\sqrt{\alpha_1 \alpha_2 / \hbar^2} \sim 302$ [m/s]. The studied dispersion is shown in Fig. 1 by a continuous line.

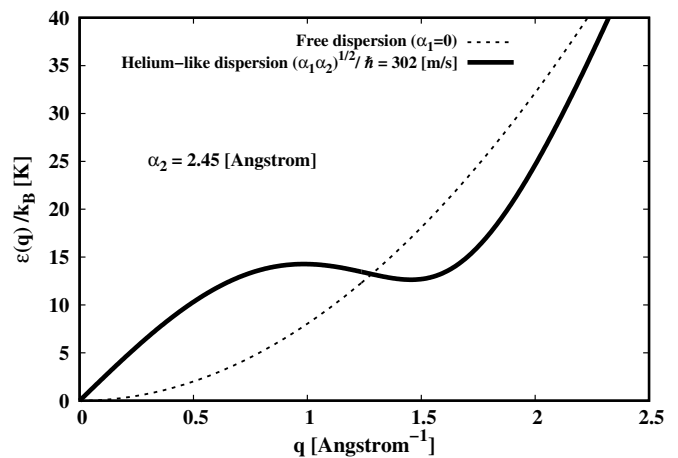


FIG. 1. Plot of the single-particle dispersions of Eq. (13) for two different α_1 parameters. The dispersion studied in this work corresponds to the continuous line.

We solved numerically Eqs. (9) and (10) fixing the density at $mN/\Omega = 0.081$ g/cm³, and report our results in Fig. 2. Notice the presence of a cusp in the curves $E_T(\xi)$ in correspondence of the critical value ξ_c . This behavior is due to the fact that the system undergoes BEC and hence a progressively larger macroscopic number of particles occupies the lowest-energy state, $\epsilon = 0$, contributing to an abrupt reduction of the average energy and a non-analytic behavior of $E_T(\xi)$.

We report in Fig. 2(b) the $\xi_E(T)$ functions, computed numerically from Eqs. (9) and (10), at energies corresponding to the critical points of the $E_T(\xi)$ curves (see Fig. 2(a)) for $T = 4, 6, 8$, and 10 K. One can see that the functions $\xi_E(T)$ are characterized by two regimes: there is a steep increase at low temperatures, until the critical point ξ_c is reached. Subsequently, the increase is less pronounced. This double regime reflects the fact that the system goes through the superfluid transition. As shown in Fig. 2(b), we found that the following function

$$\xi_E(T) = (a_0(E) + a_2(E)T^2 + a_3(E)T^3) \Theta(T - T_c) + (b_0(E) + b_1(E)T + b_2(E)T^2) \bar{\Theta}(T - T_c), \quad (14)$$

provides a good fit for the $\xi_E(T)$ curves, where T_c is the temperature of the inflection point, $\Theta(T)$ is the Heaviside function and $\bar{\Theta}(T - T_c) = (1 - \Theta(T - T_c))$. Notice that the function of Eq. (14) has the form of Eq. (6) for small T , becoming a quadratic polynomial for $T > T_c$. By solving $\xi_E(T) = -1$ one obtains the temperature T where the fermion system attains energy E .

In practice, one can compute $\xi_E(T)$ only for positive ξ , hence we re-fitted the parameters of Eq. (14) using only results in this region. We show in Fig. 2(c) (crosses), the results of the extrapolation to $\xi = -1$, compared to the actual value obtained by solving Eqs. (9) and (10) (dashed line). The agreement of the extrapolated energy

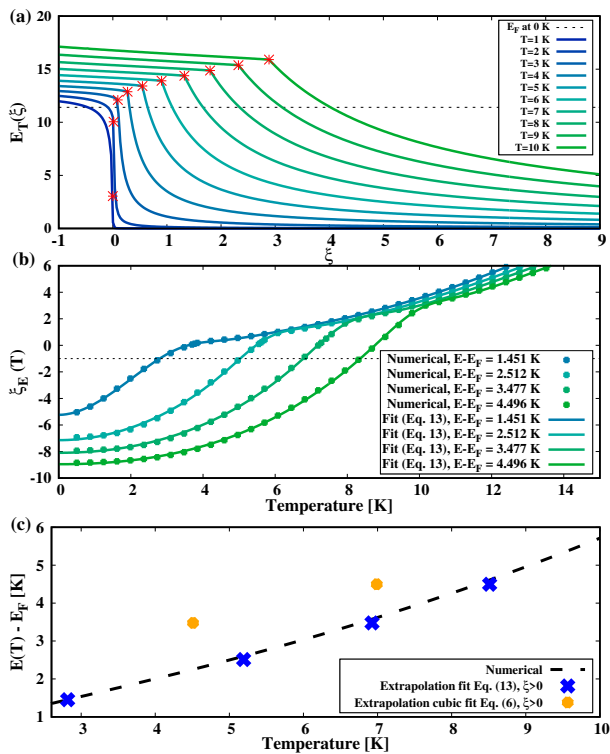


FIG. 2. (a) Energies as a function of the ξ parameter for the dispersion in Eq. (13) from Eqs. (9) and (10) for temperatures between 1 K and 10 K. Red stars indicate the energies obtained at ξ_c in Eq. (11). (b) Behaviour of $\xi_E(T)$ for a few selected energies. The latter are chosen at the critical points for $T = 4, 6, 8,$ and 10 K. Notice that the slope change of $\xi_E(T)$ is located at these temperatures. (c) Reconstructed energies as function of T . Black dashed line: numerical solution. Blue crosses: extrapolation of Eq. (14) fitted using only data for $\xi \geq 0$. Orange circles: extrapolation of Eq. (6) fitted using only data for $\xi \geq 0$.

and the actual energy is very good. In the same figure, we also show the result of the extrapolation to $\xi = -1$ using the a simple cubic form from Eq. (6), [12] fitted from the data at $\xi \geq 0$. In this case, the energy of the fermionic system is not accurately captured, and in some instances, the cubic polynomial fails to intersect the line $\xi = -1$.

IV. FINITE-SIZE EFFECTS

In the case of PIMC simulations, the results of energy calculations are generally influenced by finite-size effects.

In order to study how these limitations would affect the extrapolation to the fermion ($\xi = -1$) case, we can use the recursion formula for the canonical partition function developed in Ref. 19 for bosons and fermions, generalized

to the case of arbitrary ξ as

$$Z(N, \xi) = \frac{1}{N} \sum_{l=1}^N \xi^{l-1} S(l) Z(N-l, \xi), \quad (15)$$

where N is the number of particles and $S(l) = \sum_{i,j,k} e^{l\beta\epsilon(q_i, q_j, q_k)}$. [20, 21] In the following, we will set $N = 64$, which is the same number of particles used in the PIMC simulations of ${}^3\text{He}$.

We show in Fig. 3(a) and 3(c) the $E_T(\xi)$ curves for temperatures $T = 6$ K and $T = 8$ K, respectively. One can see that in a finite-size system the non-analytic behavior across the BEC transition is smoothed, as evidenced by the behavior of the derivative $\partial E_T / \partial \xi$ (short-dashed blue lines). Additionally, the energy per particle in the fermion case is also slightly increased with respect to the bulk value (long-dashed lines).

The finite-size smoothing of the $E_T(\xi)$ curves is mirrored into the $\xi_E(T)$ curves, as can be seen in Figs. 3(b) and 3(d) (blue triangles). The inflection due to BEC is much less evident, and finite-size effects generally flatten the $\xi_E(T)$ curve in its proximity. Nevertheless, the energy in the fermion limit ($\xi = -1$) is changed only slightly. In this case, the critical value of ξ turns out to be very close to 0, preventing a good fit with the functional form of Eq. (14). Therefore, we found it necessary to slightly change the way of extrapolating results to the fermion case. We notice that the behavior of $\xi_E(T)$ close to $\xi = 0$ is effectively linear, and hence we adopt a fitting function of the form:

$$\tilde{\xi}_E(T) = (a_0(E) + a_2(E)T) \Theta(T - T_c) + (b_0(E) + b_1(E)T + b_2(E)T^2) \bar{\Theta}(T - T_c), \quad (16)$$

where T_c is estimated as the temperature after which the non-linear form of $\xi_E(T)$ is apparent. We stress that the linear term in Eq. (16) is not meant to describe the physics for $T \rightarrow 0$, where ξ_E can take values well below -1 , but only as a simple and effective extrapolation method to $\xi = -1$. Notice that the $\xi_E(T)$ curves show an evident linear behavior close to $\xi = 0$ even in the bulk model.

In Figures 3(b) and 3(d) the red dashed line represents the fit using Eq. (16) taking into account only $\xi_E \geq 0$ finite size points, while the green continuous curve is the fit taking into account the points for which $\xi_E \geq -1$. Notice that the linear extrapolation introduces a slight uncertainty in the order of 0.1 K in the position of the temperature where $\xi = -1$ is crossed.

V. PIMC RESULTS FOR ${}^3\text{He}$

In the case of ${}^3\text{He}$ simulations, we used the PIMC approach [15, 23] to sample the partition function and the worm algorithm to sample permutations. [24] Details of PIMC algorithm are presented elsewhere. [25, 26] The only modification to the original set of MC moves,[25] is

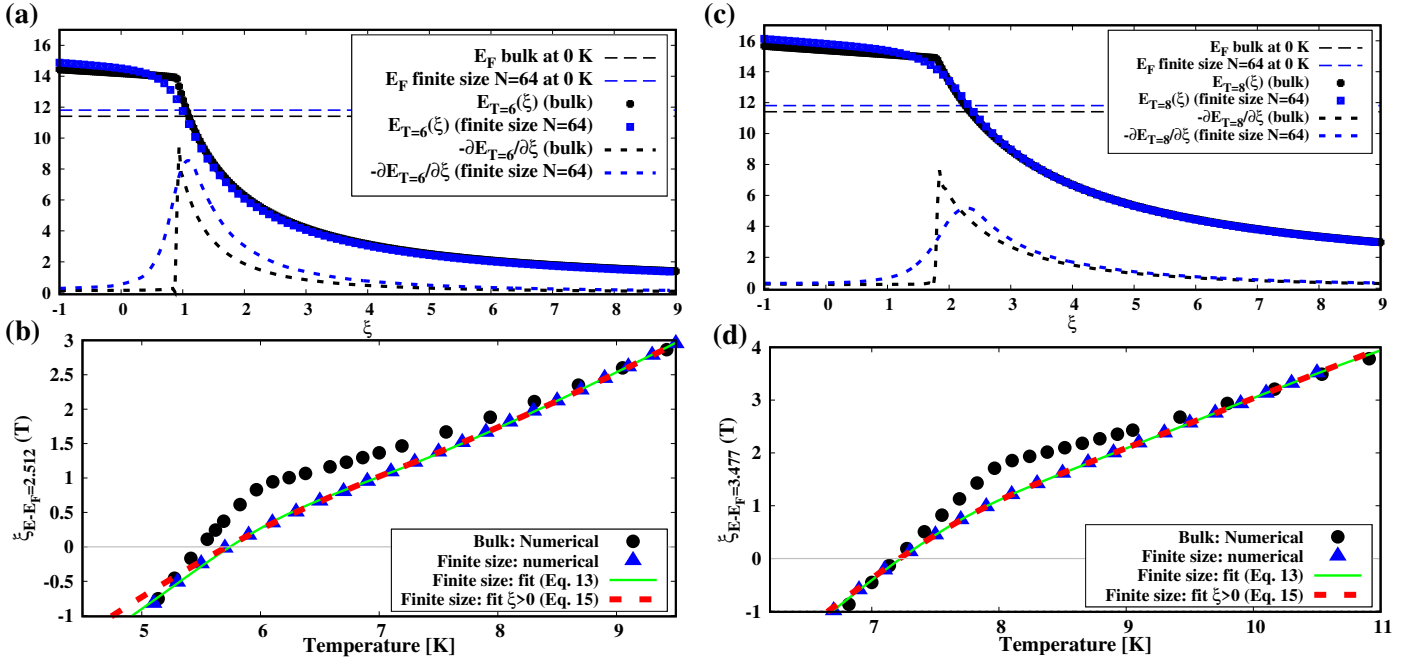


FIG. 3. (a) Comparison of the energy and its derivative with respect to ξ for $T = 6$ K for the bulk system (black points and black short-dashed line) and the finite size system (blue points and blue dashed-line). The long-dashed lines are located at the Fermi level of the bulk (black) and finite system (blue). (b) Comparison of $\xi_E(T)$ for $E - E_F = 2.512$ K for the bulk system (black circles) versus the finite system (blue triangles). This value for the energy is chosen at the ξ_c of the bulk system in (a). (c) Same as (a) but for $T = 8$ K. (d) same as (b) but at the critical point of (c), corresponding to an energy of $E - E_F = 3.477$ K.

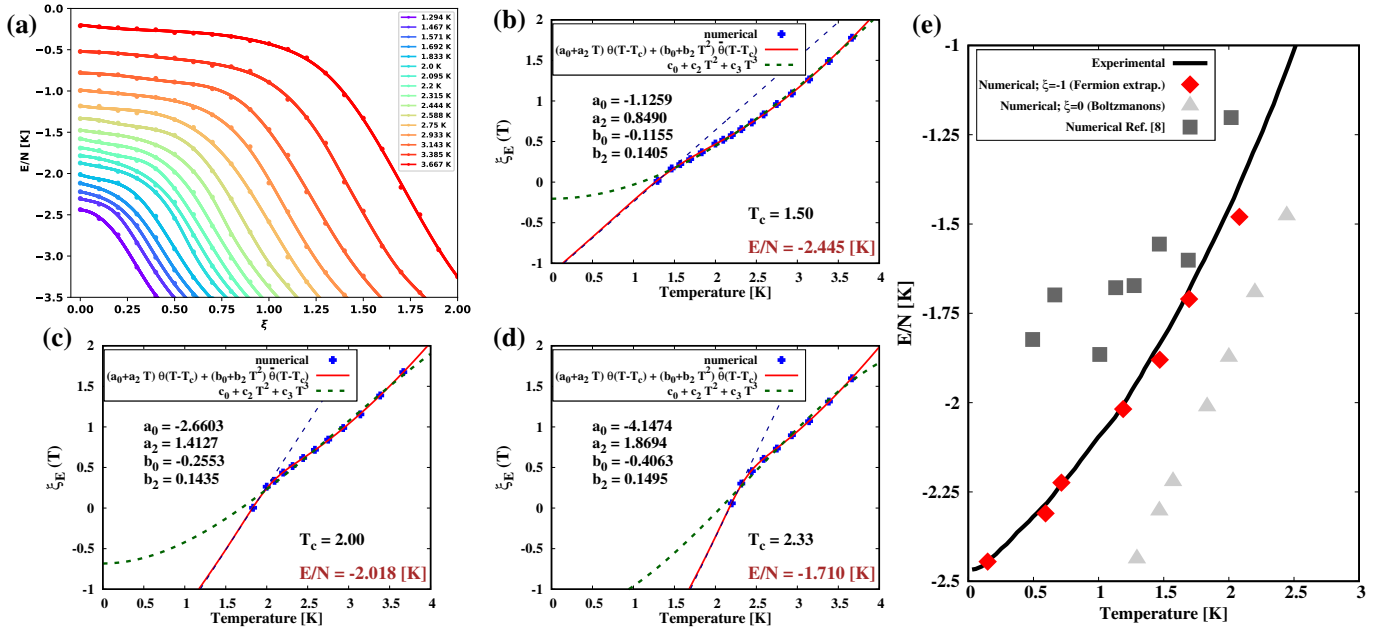


FIG. 4. ^3He results. (a) Energy as a function of the ξ parameter for temperatures T in the range of (1.294, 3.667) K. (b-d) $\xi_E(T)$ for four different energies per particle. We report the values of the fit using Eq. (16) (red lines), the linear fit passing through the points for $\xi \sim 0$ (dark-blue dashed lines) and the cubic fit using Eq. (6) (dark-green dashed lines). (e) Total energy per particle as a function of temperature. Black line corresponds to the experimental data from Ref. [22]; red points are the one extrapolated to $\xi = -1$, light-gray triangular points are the $\xi = 0$ (Boltzmanns) energies while dark-gray square points are the numerical results obtained using PIMC plus fixed-node approximation in Ref. [8].

the one including the ξ factor of Eq. (2) in the weight factor of the *swap* move, the one responsible for the exchange permutation sampling. We considered a system of $N = 64$ atoms at a density $\rho = 0.016355$ atoms/Å³, using periodic boundary conditions. We employed the most recent *ab-initio* two-body potential to treat the interaction between ³He atoms [27] and we evaluated the propagator in the pair-product approximation [28] with fixed $\tau = \frac{\beta}{P} = \frac{1}{44}$ K⁻¹, where P is the number of beads (imaginary-time slices) of the PIMC approach. For each temperature, P is thus chosen as $P = \text{int}[\frac{1}{\tau T}]$, where $\text{int}(x)$ is the closest integer number to x . Energies are estimated using the virial estimator [15] and then are corrected perturbatively by adding the three-body potential contribution. [29] Results for ³He are shown in Fig. 4. Panel (a) reports the energies obtained as a function of the ξ parameter at temperatures ranging from 1.294 K to 3.667 K. The points obtained from PIMC calculations are interpolated using B-splines. [30] The behaviour of the $E_T(\xi)$ closely resembles the finite size calculations using the helium-like dispersion of Eq. (13), with a T -dependent smoothed inflection point where the superfluid transition occurs. In Figs. 4(b-d) we show three $\xi E(T)$ functions, estimated by cutting the curves in Fig. 4(a) at constant energies. Blue points represent numerical data, while the red lines are the fits using Eq. (16). For the sake of reproducibility, the values of the parameters are reported in those figures. The dark-green dashed lines represent fits using a simple cubic polynomial, as used in the original papers on this method; [12] Notice that in some cases (panels (b) and (c)), this fitting function does not intersect the $\xi = -1$ line, which leads to an unphysical result: it would imply that no temperature corresponds to the assumed value of the energy per particle.

Finally, we show in Fig. 4(e) and Table I the results for the energy per particle obtained by extrapolation of the fitting function in Eq. (16). The experimental results from Ref. 22 are in remarkably close agreement with our findings. In Fig. 4(e), we also report the energy per particle without exchange effects (Boltzmanns, that is

$\xi = 0$) and the results obtained using PIMC in conjunction with a fixed-node constraint: [8] the former strongly underestimate the fermion energies, while the latter are closed to the experimental value, but display a more scattered behavior.

E/N [K]	T [K] Extrapol. $\xi = -1$	T [K] Boltzmann. $\xi = 0$
-2.445	0.149	1.294
-2.310	0.593	1.467
-2.224	0.714	1.571
-2.018	1.189	1.833
-1.880	1.470	2.000
-1.710	1.694	2.200
-1.480	2.081	2.444

TABLE I. Summary of the numerical energies and temperatures reported in Fig. 4(e). All the energies are given in Kelvin units.

VI. CONCLUSIONS

In this paper, we presented simulations of normal liquid ³He where the fermionic nature of the system was taken into account using a recently developed approach based on a ξ -parametrized partition function that continuously interpolates between bosonic ($\xi = 1$) and fermionic ($\xi = -1$) statistics. We found that the presence of the superfluid transition in the $\xi > 0$ sector, where calculations were not affected by the sign problem, induced significant non-analytic behavior in the function $E(T, \xi)$ that required a tailored approach to extrapolate to the fermion case. Our simulations yielded very good agreement with experimental data for the energy of particles. The approach developed here may find useful application in other strongly-interacting fermionic systems, such as those relevant to nuclear physics.

ACKNOWLEDGEMENTS

TM and GG thank Gabriele Spada and Stefano Giorgini for useful discussions and for the details of the PIMC+worm algorithm.

-
- [1] A. Szabo and N. S. Ostlund, *Modern quantum chemistry: introduction to advanced electronic structure theory* (Courier Corporation, 2012).
 - [2] R. J. Bartlett and M. Musiał, Coupled-cluster theory in quantum chemistry, *Reviews of Modern Physics* **79**, 291 (2007).
 - [3] E. Y. Loh, J. E. Gubernatis, R. T. Scalettar, S. R. White, D. J. Scalapino, and R. L. Sugar, Sign problem in the numerical simulation of many-electron systems, *Phys. Rev. B* **41**, 9301 (1990).
 - [4] E. Lipparini, *Modern many-particle physics: atomic gases, nanostructures and quantum liquids* (World scientific, 2008).
 - [5] T. Dornheim, Fermion sign problem in path integral Monte Carlo simulations: Quantum dots, ultracold atoms, and warm dense matter, *Phys. Rev. E* **100**, 023307 (2019).
 - [6] T. Dornheim, Z. A. Moldabekov, J. Vorberger, and B. Militzer, Path integral Monte Carlo approach to the structural properties and collective excitations of liquid ³He without fixed nodes, *Scientific Reports* **12**, 708 (2022).
 - [7] J. B. Anderson, A random-walk simulation of the Schrödinger equation: H₃⁺, *The Journal of Chemical Physics* **63**, 1499 (1975).
 - [8] D. M. Ceperley, Path-integral calculations of normal liquid ³He, *Phys. Rev. Lett.* **69**, 331 (1992).

- [9] K. Nakano, C. Attaccalite, M. Barborini, L. Capriotti, M. Casula, E. Coccia, M. Dagrada, C. Genovese, Y. Luo, G. Mazzola, A. Zen, and S. Sorella, TurboRVB: A many-body toolkit for ab initio electronic simulations by quantum Monte Carlo, *The Journal of Chemical Physics* **152**, 204121 (2020).
- [10] T. Dornheim, P. Tolias, S. Groth, Z. A. Moldabekov, J. Vorberger, and B. Hirshberg, Fermionic physics from ab initio path integral Monte Carlo simulations of fictitious identical particles, *The Journal of Chemical Physics* **159**, 164113 (2023).
- [11] Y. Xiong and H. Xiong, On the thermodynamic properties of fictitious identical particles and the application to fermion sign problem, *The Journal of Chemical Physics* **157**, 094112 (2022).
- [12] Y. Xiong and H. Xiong, Thermodynamics of fermions at any temperature based on parametrized partition function, *Phys. Rev. E* **107**, 055308 (2023).
- [13] T. Dornheim, S. Schwalbe, M. P. Bohme, Z. A. Moldabekov, J. Vorberger, and P. Tolias, Ab initio path integral Monte Carlo simulations of warm dense two-component systems without fixed nodes: Structural properties, *The Journal of Chemical Physics* **160**, 164111 (2024).
- [14] T. Dornheim, S. Schwalbe, Z. A. Moldabekov, J. Vorberger, and P. Tolias, Ab initio path integral Monte Carlo simulations of the uniform electron gas on large length scales, *The Journal of Physical Chemistry Letters* **15**, 1305 (2024).
- [15] D. M. Ceperley, Path integrals in the theory of condensed helium, *Rev. Mod. Phys.* **67**, 279 (1995).
- [16] S. Isakov, Generalization of quantum statistics in statistical mechanics, *International journal of theoretical physics* **32**, 737 (1993).
- [17] L. Pitaevskii and S. Stringari, *Bose-Einstein condensation and superfluidity*, Vol. 164 (Oxford University Press, 2016).
- [18] M. Lemeshko and R. Schmidt, Molecular Impurities Interacting with a Many-particle Environment: From Ultracold Gases to Helium Nanodroplets, in *Cold Chemistry: Molecular Scattering and Reactivity Near Absolute Zero* (The Royal Society of Chemistry, 2017).
- [19] P. Borrnann and G. Franke, Recursion formulas for quantum statistical partition functions, *The Journal of Chemical Physics* **98**, 2484 (1993).
- [20] B. Hirshberg, V. Rizzi, and M. Parrinello, Path integral molecular dynamics for bosons, *Proceedings of the National Academy of Sciences* **116**, 21445 (2019).
- [21] B. Hirshberg, M. Invernizzi, and M. Parrinello, Path integral molecular dynamics for fermions: Alleviating the sign problem with the Bogoliubov inequality, *The Journal of Chemical Physics* **152**, 171102 (2020).
- [22] D. S. Greywall, Specific heat of normal liquid ^3He , *Phys. Rev. B* **27**, 2747 (1983).
- [23] D. M. Ceperley and E. L. Pollock, Path-integral computation of the low-temperature properties of liquid ^4He , *Phys. Rev. Lett.* **56**, 351 (1986).
- [24] M. Boninsegni, N. Prokof'ev, and B. Svistunov, Worm algorithm for continuous-space path integral Monte Carlo simulations, *Phys. Rev. Lett.* **96**, 070601 (2006).
- [25] G. Spada, S. Giorgini, and S. Pilati, Path-integral Monte Carlo worm algorithm for Bose systems with periodic boundary conditions, *Condensed Matter* **7** (2022).
- [26] T. Morresi and G. Garberoglio, Revisiting the properties of superfluid ^4He using fully *ab initio* potentials, in preparation.
- [27] P. Czachorowski, M. Przybytek, M. Lesiuk, M. Puchalski, and B. Jeziorski, Second virial coefficients for ^4He and ^3He from an accurate relativistic interaction potential, *Phys. Rev. A* **102**, 042810 (2020).
- [28] E. L. Pollock and D. M. Ceperley, Simulation of quantum many-body systems by path-integral methods, *Phys. Rev. B* **30**, 2555 (1984).
- [29] J. Lang, G. Garberoglio, M. Przybytek, M. Jeziorska, and B. Jeziorski, Three-body potential and third virial coefficients for helium including relativistic and nuclear-motion effects, *Phys. Chem. Chem. Phys.* **25**, 23395 (2023).
- [30] P. Dierckx, An algorithm for smoothing, differentiation and integration of experimental data using spline functions, *Journal of Computational and Applied Mathematics* **1**, 165 (1975).